High resolution topography of Titan adapting the Delay-Doppler algorithm to the Cassini RADAR Altimeter Data

Valerio Poggiali, Marco Mastrogiuseppe, Alexander G. Hayes, Roberto Seu, Joseph Peter Mullen, Samuel Patrick Dennis Birch and Maria Carmela Raguso

***Abstract*— The Cassini RADAR altimeter has provided broad-scale surface topography data for Saturn's largest moon Titan. Herein, we adapt the Delay-Doppler algorithm to take into account Cassini geometries and antenna mispointing usually occurring during hyperbolic Titan flybys. The proposed algorithm allows up to tenfold improvement in the along-track resolution. Preliminary results are provided that show how the improved topography presented herein can advance our understanding of Titan's surface characteristics.**

***Index Terms*—Radar, Spaceborne Radar, Radar Altimetry, Radar Signal Processing, Delay/Doppler Algorithm, Planetary Science, Cassini, Titan.**

I. Introduction

The Cassini RADAR is a multimode Ku-band (13.78 GHz) radar instrument [1] that provided topographic information of the surface of Saturn's largest moon, Titan, from 2004 to 2017 (see Table 1, instrument parameters). During the course of its mission, the Cassini spacecraft performed a total of 127 flybys of Titan, activating the altimetric mode [2; 3; 4] during 40 of them (see Table 1, zonal distribution). In Table 2 we report the whole Cassini dataset of altimetric acquisitions with the best ground resolution achieved in along track during each flyby and the most important surface features [5] observed from Cassini Synthetic aperture radar (SAR) mapping. SAR mode, indeed, has been able to provide imaging at ≤300 m/pixel of ~20% of the surface (~50% at ≤1500 m/pixel). Other modes of the radar, not dealt with in this paper, enabled the measurement of microwave thermal energy emitted by the surface (radiometry) and the acquisition of low-resolution backscatter images (scatterometry).

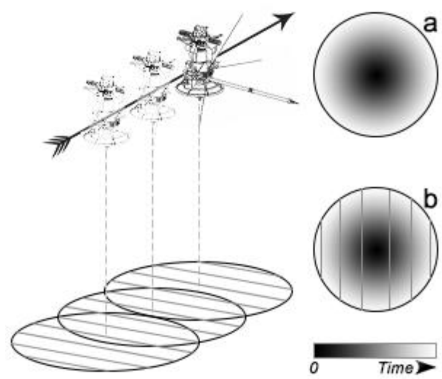

Fig. 1. Delay/Doppler altimetry: geometry of acquisition. (a) Conventional radar altimetry estimates the distance between radar and underlying surface by averaging all the echoes returning from the footprint. (b) Delay/Doppler altimetry exploits Doppler selectivity to discriminate echoes returning from different cells along-track, thus enabling an extra dimension in the measurement space.

The specific geometry of Cassini acquisitions (hyperbolic), caused the range of spacecraft altitudes to span up to several thousand kilometers along a single altimetric track. This wide range of altitudes caused in turn the ground resolution to significantly vary during each flyby.

Doppler processing techniques have been demonstrated to greatly improve the performances of conventional radar altimeters for terrestrial applications as well as planetary purposes. For example, Doppler beam sharpening is a well-known powerful technique that greatly increases the along-track resolution of altimetric data [6; 7].

Doppler-resolved altimetry processing allows non-coherent integration of the overlapped Doppler bins (see Fig. 1) by compensating time delay offsets due to the different paths travelled by signals to reach the same frequency-resolved surface footprints. This technique was originally applied to radar data from the Magellan mission to Venus, revealing much more details of the surface [6] and obtaining up to a seven times enhancement of the along-track resolution.

Based on the same principle, [8] introduced the Delay-Doppler algorithm (DDA) used today in terrestrial radar applications, such as the Cryosat-2, AltiKa, and Sentinel-3 missions

Submitted for review on 11/19/2018.

V.P., A.G.H. acknowledge funding for this work from the NASA PDART program grant number 80NSSC18K0513 and NASA CDAP program grant number NNX15AH10G.

S.P.D.B. acknowledges funding for this work from the NASA NESSF program grant number NNX15AQ87H.

R.S. acknowledges funding for this work by ASI from Grant Number 2017-10-H.0.

V.P., A.G.H., J.M. and S.P.D.B. are with the Department of Astronomy, Cornell University, Ithaca, New York, USA. (e-mail: vp226@cornell.edu, hayes@astro.cornell.edu, joseph.p.mullen@drake.edu and sb2222@cornell.edu).

R.S. is with the Dipartimento di Ingegneria dell'Informazione, Elettronica e Telecomunicazioni, Università di Roma "La Sapienza", Roma, Italy. (e-mail: roberto.seu@uniroma1.it).

M.M. and R.S. are with the Geology and Planetary Science Division at the California Institute of Technology (Caltech), Pasadena, CA, USA. (e-mail: mmastrog@caltech.edu and mraguso@caltech.edu).

(e.g., [9; 10]). The DDA is also crucial to ESA's COASTAL and SAMOSA projects for coastal monitoring, where the increased spatial resolution is allowing the recovery of large quantities of otherwise discarded data acquired near coastlines and on inland waters [11].

This paper describes how to implement the delay/Doppler algorithm to the specific case of the Cassini radar altimeter data. The algorithm is adapted to take into account the hyperbolic geometry of Cassini spacecraft and the antenna mispointing (θ_{off}) that usually occurs during Titan flybys (see Table 1, antenna mispointing).

TABLE I

RADAR INSTRUMENT PARAMETERS				
Wavelength (λ) = 2.17 cm				
Chirped signal duration (τ) = 150 µs				
Chirped signal bandwidth (B) = 4.25 MHz				
Burst repetition interval (BRI) = 0.5/4 s				
Number of pulses within each burst (N_{RX}) = 15				
Pulse repetition frequency (PRF) = 5 kHz				
Peak transmitted power (P_{TX}) = 40.084 W				
Antenna -3dB beamwidth (θ_{3dB}) = 6.1 mrad				
Peak antenna gain (G_0) = 50.7 dB				
Spacecraft altitude in altimetry mode (H) = 1000 to 9000 km				
Spacecraft tangential velocity (v_t) = 2/6 km/s				
Spacecraft radial velocity (v_{rad}) = 0/5.2 km/s				
ZONAL DISTRIBUTION (±45° BORDERS)				
Area of Titan	North	Equator	South	
Dataset %	17	78	5	
ANTENNA MISPOINTING				
θ_{off}(°)	θ<0.01	0.01<θ<0.04	0.04<θ<0.2	θ >0.2
Dataset %	29	28	40	3

An interested reader could also refer to [4] for a non-coherent model of the average impulse response of a rough surface that has been developed for the Cassini radar altimeter.

II. DELAY/DOPPLER PROCESSING ADAPTED TO CASSINI RADAR ALTIMETER DATA

The along-track resolution achievable by a delay-Doppler algorithm [8] is given by

$$\delta \mathrm{d} = \frac{\mathrm{H} \cdot \lambda \cdot \mathrm{PRF}}{2 \cdot \mathrm{v_t} \cdot N} \qquad (1)$$

with H the spacecraft altitude, λ the transmitted signal wavelength, $\mathrm{v_t}$ the spacecraft tangential velocity and N is the number of Doppler filters useful for the processing, that can be expressed by:

$$N = \frac{B_D}{\delta f} \qquad (2)$$

with $B_D = 2\,\mathrm{v_t} \sin(\varphi)/\lambda$ the Doppler bandwidth, $\delta f = \mathrm{PRF}/N_{RX}$ the Doppler resolution, N_{RX} the total number of echoes received within the burst (or the number of available filters), φ an integration angle depending on spacecraft altitude and encompassing the antenna aperture from which echo power is received (see appendix of [6] for more details).

Figure 2 shows the complete block diagram of the DDA applied to the Cassini radar altimeter data. The main steps of the proposed processing are:

TABLE II
ALTIMETRY DATASET (TA-T126) AND SURFACE UNITS OBSERVED

Swath Name	Day	Number of Alt. Bursts	Min. Real-Aperture Footprint [km]	Landforms in Track
Ta	26/10/2004	458	31	HM; CR;
T3	15/02/2005	291	36	HM; DU;
T8	28/10/2005	742	31	DU; HM;
T13	30/04/2006	268	34	DU;
T16	21/07/2006	886	32	HM; DU;
T19	9/10/2006	911	31	BP;
T20	25/10/2006	20	81	BP
T21	12/12/2006	444	35	DU;
T23	13/01/2007	887	31	BP; PL;
T25	22/02/2007	57	32	HM;
T28	10/4/2007	1248	33	PL; HM;
T29	26/04/2007	982	33	HM; PLS;
T30	12/5/2007	3439	6	HM; DU; PL; EL; MO;
T36	2/10/2007	1833	34	HM; DU; PL;
T39	20/12/2007	633	34	HM; DU; PL;
T41	22/02/2008	398	7	HM; MO; PLS;
T43	12/5/2008	590	35	PL;
T44	28/05/2008	654	30	BP; MO;
T48	5/12/2008	130	33	NCBS;
T49	21/12/2008	912	8	MO; FL; RI;
T50	7/2/2009	404	28	HM; PL;
T55	21/05/2009	637	33	BP;
T56	6/6/2009	261	32	HM; PL; BP;
T57	22/06/2009	562	26	NCBS; PLS;
T61	25/08/2009	133	31	DU;
T64	27/12/2009	586	30	HM; DU;
T77	20/06/2011	1688	8	DU; PL; BP;
T83	21/05/2012	626	30	HM; CR; DU; BP;
T84	6/6/2012	626	31	BP;
T86	26/09/2012	61	38	HM; BP;
T91	23/05/2013	1335	6	DU; BP; EL; FL; RI;
T92	10/7/2013	280	31	FL;
T95	14/10/2013	212	31	FL;
T98	2/2/2014	2236	8	HM; DU; BP; MO; PLS;
T104	21/08/2014	645	10	FL;
T108	11/1/2015	456	6	HM; DU; BP; EL; FL; RI;
T113	28/09/2015	204	31	DU; BP;
T120	7/6/2016	290	30	DU; BP;
T121	25/7/2016	292	30	CR;
T126	22/4/2017	472	7	PL; EL; FL;

HM: inselbergs/hummocks; CR: craters; DU: dunes; BP: bright planes; PL: planes; EL: empty lakes; FL: filled lakes; RI: rivers; MO: mountains; PLS: possible liquid surface; NCBS: not covered by SAR.

a) extraction of ancillary data and range compression executed during conventional processing of the altimetric data (for a detailed description please see [3; 12; 13]);
b) phase shift compensation due to the radial velocity variations experienced by the spacecraft during its hyperbolic Titan flybys and to the antenna mispointing;
c) along-track Discrete Fourier Transform (DFT) is performed to pass into the range - Doppler domain. Weighting windows are applied here to mitigate sidelobes;
d) (optional step) application of a super-resolution technique in range (i.e., see [14]);
e) range-delay compensation taking into account the spacecraft attitude (i.e. off-nadir angle);
f) antenna gain pattern compensation;

g) incoherent average of Doppler cells;
h) altimetry profiles generation.

After the extraction of ancillary data and range compression (step a), we compensate the phase shift caused by the spacecraft radial velocity (step b) by multiplying the Cassini burst for:

$$\Omega(\mathrm{t}') = \exp\left\{-j\,\frac{4\pi \cdot v_{rad} \cdot t'}{\lambda}\right\} \tag{3}$$

with v_{rad} the spacecraft radial velocity and t' is the slow-time, indicated as a discrete intra-burst time vector defined as n/PRF, with $n = 1{:}\,N_{RX}$.

The 4.25MHz chirp bandwidth of the Cassini RADAR altimeter allows production of relative elevation profiles with a vertical resolution of 35 m. However, studies performed by [14] concerning the application of parametric autoregressive (AR) time-series models revealed the possibility to improve the range resolution of the radar by a factor of up to x3. This method has been successfully adopted by Mastrogiuseppe et al. [15, 16, 17] on Cassini, and by Raguso et al. [18; 19] on SHARAD and MARSIS data. These works demonstrated that the application of parametric AR time-series models (i.e., Burg's Maximum Entropy Method) can effectively be used to improve range resolution of coherent radar returns with the advantage that the linearity of this kind of processes makes recompressed pulses still suitable for backscattering and phase responses studies [14]. The discretionary implementation of this step of processing (step d) can include the application of any super-resolution technique in range just after performing the DFT in along-track (step c).

The key-step of the delay-Doppler processing is the compensation of the range-delay associated to all the filters of the azimuthal Fourier transform and relative to different along-track positions (step e). The goal of this operation is to allow signals to have the same range when the successive step of incoherent integration will be executed.
In frequency domain these delays correspond to constant (CW) frequency shifts that can be compensated by multiplying the signal content at each Doppler position (f') by an equal and opposite range CW signal [8]:

$$\Phi(f', t) = \exp\left\{+j\,\frac{4\pi \cdot k \cdot \delta r(f') \cdot t}{c}\right\} \tag{4}$$

with

$$\delta r(f') \cong \alpha_R\,\frac{\lambda^2 {f'}^2 H}{8\,{v_t}^2} \tag{5}$$

where k is the chirp rate, c is the speed of light and $\alpha_R \cong R_T/(R_T + H)$ is Titan's surface curvature [4], and t the fast-time. In this context, the frequency in range is proportional to the delay respect to the altimeter tracking-point and the frequency in along-track is indicative of relative position of a scatterer respect to the zero-Doppler point. In our work, the formula (5) is calculated according to the antenna mispointing angle of the observation (along track component or pitch angle), which is recorded into the Cassini SPICE kernels. Antenna mispointing causes an additional increment of delay due to

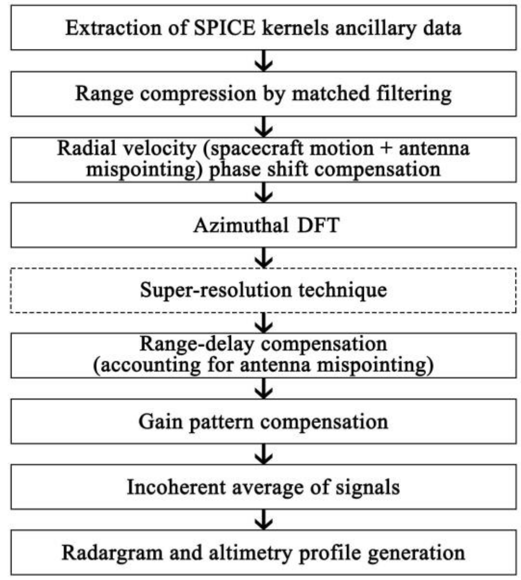

Fig. 2. Delay/Doppler processing work-flow adapted for the Cassini mission.

the Doppler frequency shift introduced. While this Doppler shift is compensated in step b, the delay increments are calculated taking into account the actual Doppler frequency (f') of each bin at the time of observation. The additional increment of frequency (f_D) is calculated from off-nadir and is added to the Doppler frequency calculated at nadir (f):

$$f' = f - f_D \tag{6}$$

with

$$f_D = \frac{2 \cdot v_t \cdot \sin\theta_{off}}{\lambda} \tag{7}$$

The compensation of antenna gain pattern is performed (step f) by considering a gaussian antenna beam:

$$G(f) \approx G_0 \exp\left\{-\frac{1}{2\gamma}\left(\frac{\lambda \cdot f}{v_t}\right)^2\right\} \tag{8}$$

with

$$\gamma = -\frac{2\,\sin^2(\theta_{3dB}/2)}{\ln 0.5} \tag{9}$$

Note that the gain pattern compensation is accomplished by applying a signal adaptive 2-D mask able to compensate the gain effects when signal is present. Specifically, the noise is evaluated and only signal having a Signal-to-Noise Ratio (SNR)>10dB is compensated for gain. This allows to avoid gain compensation of noise pixels, similarly to what is done for the Cassini SAR images processing [20].
Finally, we sort the individual Doppler components from subsequent, but different, bursts in order to perform their incoherent average (step g). This operation is performed by locating the Doppler cells on the (spherical) surface of Titan and calculating their relative orthodromic distance by means of the geographical information contained in the Cassini SPICE kernels. At this point, a high resolution radargram is generated (step h).

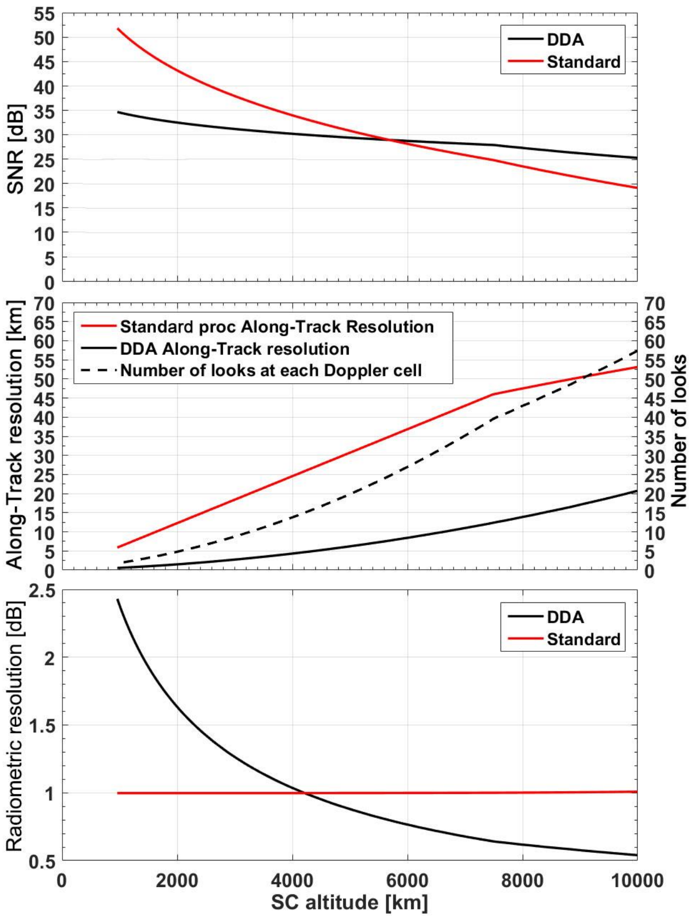

Fig. 3. (top) Delay/Doppler vs Standard processing: SNR obtained with BRI = 0.5 s and σ^0 = 0 dB; (middle) Improvement in along-track resolution given by the delay-Doppler (black solid line) in comparison with the standard processing (red solid line); with a black dashed line is indicated the number of looks at each Doppler cell. Note the variation in slope at 7500 km due to the switch from beam- to pulse-limited mode; (bottom) Radiometric resolution vs Spacecraft altitude obtained with BRI = 0.5 s and σ^0 = 0 dB for both the Delay-Doppler and Standard processing.

The backscattering values of DDA products is calculated inverting the radar equation:

$$P_{RX} = \frac{P_{TX} G_0^2 \lambda^2 B\tau}{(4\pi)^3 H^4} \sigma^0 A\ K\ N_L \qquad (11)$$

where P_{RX} is the received power, $B\tau$ is the compression gain in range; σ^0 is the normalized backscattering coefficient of the terrain (dimensionless); A is the area of the Doppler footprint that has a cross-track dimension equal to the diameter of the beam-/pulse-limited antenna footprint (i.e. -3dB aperture) and an along-track dimension that can be approximated for convenience by δd; N_L is the number of looks at each Doppler position (conveniently stored in a counter variable during the processing). Note that at the beginning of any altimetric observation of the Cassini radar, a calibration routine is performed by pointing the antenna to the cold sky and relating the measured noise power to its theoretical thermal noise equivalent. The calibration is needed to determine an analog-to-digital conversion parameter between the value of digitized watts, at the output of the radar receiver, and true watts. In our formula, $K = \mathrm{C}/\mathrm{L}$ accounts for this calibration parameter C and the flyby receiver attenuator value L, the latter adopted to keep the echo amplitude on-scale and avoid saturation [21];

The middle panel of Figure 3 shows the significative improvement in along-track resolution given by the DDA (black solid line) in comparison with the along-track resolution achieved by the conventional altimetric processing (red solid line), for spacecraft altitudes varying from 1000 to 10000 km. For example, in the case of nominal altitudes 1000 - 9000 km, the DDA increases the resolution by a factor ranging from 10 to 3 with respect to the conventional processing.

The top panel of Figure 3 shows the comparison between values of SNR obtained applying the DDA (black line) and the standard processing (red line). A slight improvement in SNR and in radiometric resolution (Fig. 3, bottom panel) are observed only at the higher altitudes, where a larger number of looks is available (black dashed line, middle panel of Fig. 3) with respect to the standard processing (N_{RX} = 15).

The high values of SNR obtained at nominal altitudes by both the processings cause the precision in height estimation to be not significantly affected: i.e., when observing surfaces with 20 m height standard deviation, the precision in range is always better than 8 m.

III. Results

A detailed knowledge of Titan's surface topography is currently lacking. Available topographic data (DTMs and SAR-Topo) have a vertical resolution of ~50 m at best (~150 m on average), with horizontal resolutions on the order of several kilometers. While this provides a coarse knowledge of the topography, it is currently not possible to resolve the key geologic features, such as dunes or fluvial valley networks, that would constrain the dominant processes that transport material across Titan's surface.

With the more effective use of the altimetry dataset that we propose, we can improve topography and knowledge of geologic features distributed across the surface of Titan, resulting in a better understanding of Titan's history and surface evolution.

Hereafter, we will provide two case studies over specific geomorphic units including hummocks and empty lake basins.

A. Hummocky terrains are SAR-bright, topographic highs that are interpreted to represent the oldest geologic terrains on Titan [5]. The SAR image in Figure 4 (panel 'e') was acquired during the Cassini T43 flyby of Titan (5/12/2008) and shows an area in the north-eastern part of Titan's Dilmum region (19.8° N, 163.7° W) which is dominated by the presence of isolated patches of higher SAR backscatter, identified as degraded hummocky terrains units within a SAR-dark undifferentiated plain. On 2/2/2014 the Cassini spacecraft executed a new flyby of Titan (T98) during which the same hummocky region was re-observed by the radar instrument in altimetry mode from an altitude of 2600 km. The areal extent of individual hummocks was generally smaller than any given -3dB altimetric footprint (16 km in diameter), but the x7 improvement in the along-track resolution (~2.2 km Doppler cell) respect to the conventional product (Figure 4, panels ‘a’) manifests the capability of the DDA to reveal the presence of new features (Figure 4, panels ‘b’), which have a direct correspondence with the radar bright features shown by SAR images (Fig. 4, panel ‘e’). We applied two different height estimators over the returned echoes: Threshold and First-Moment [22]. These trackers are sensible to the most elevated portions of the surface and to the average height within the Doppler footprint respectively. The application of the threshold tracker spatially resolves individual hummocks and indicates the heights of these structures to be in the order of ~300 meters (Figure 4, panel ‘c’).

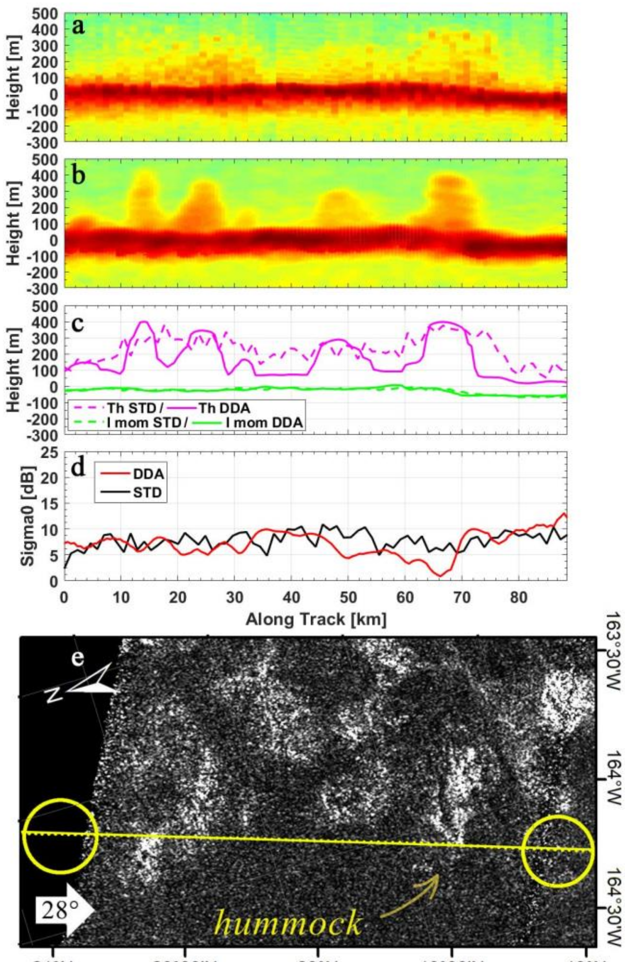

Fig. 4. Hummocks as seen by delay/Doppler radar altimeter. It is hard to isolate their topographic characteristics with conventional radar altimetry: their height contribute is averaged on the wider footprint scale. Thanks to a more effective use of the received power, the delay/Doppler altimetry can determine topographic characteristics of these previously unresolved features. **(a)** 73 bursts from T98 altimetry radargram obtained with conventional altimetry. **(b)** radargram obtained with Delay/Doppler altimetry processing. **(c)** I moment (I mom) and Threshold (Th) height estimators’ altimetry profiles: solid and dotted lines respectively show results obtained for delay/Doppler and standard processing. **(d)** received backscatter at nadir before (black) and after delay/Doppler processing (red). **(e)** T43 SAR image of the region of interest with the spacecraft ground track (yellow line) and the -3dB footprints (yellow circles), both aligned with the altimetric profiles shown in the upper panels.

B. Empty lake basins are a geologic feature unique to Titan. Restricted to the polar regions, the lakes form closed depressions (at the coarse resolution of Cassini’s SAR images) that are hundreds of meters deep and have high-sloping interior walls [23; 24]. During the flyby T28 of Titan (4/10/2007) the Cassini radar acquired a long SAR image strip ranging from the equatorial area 15°S to the northern seas 79°N. In Figure 5 (panel ‘e’) it is shown the SAR image of the 30 x 40 km empty lake basin (69.5°N, 5°E) that was observed in that occasion, crossed by the flyby T30 altimetric track acquired about one month later (5/12/2007) from an altitude of 960 km. While the diameter of the beam limited antenna footprint in this case is of ~6 km, the DDA here ensures an along track resolution of ~560 m, corresponding to a tenfold improvement. An analysis of available topographic data for Titan’s lakes shows that the larger depressions have hundreds-meter high raised rims, often offset by hundreds of meters on opposite sides of the same lake [25; 24]. While conventional altimetry can only roughly describe their topography, the Doppler-resolved altimetry is

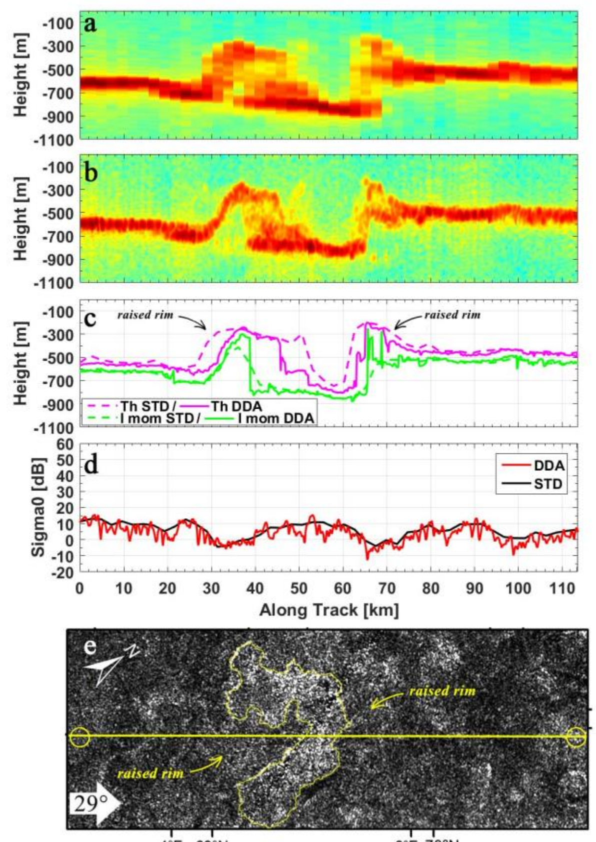

Fig. 5. An empty lake basin as seen by delay/Doppler radar altimeter. **(a)** 50 bursts from T30 altimetry radargram obtained with conventional altimetry. **(b)** radargram obtained with Delay/Doppler altimetry processing. **(c)** I moment (I mom) and threshold (Th) topographic profiles. **(d)** received backscatter at nadir before (black) and after delay/Doppler processing. **(e)** T28 SAR image of the region with -3dB altimetric footprints (yellow circles) and the profile’s ground-track (yellow line). The perimeter of the empty lake of interest is also highlighted with a thinner yellow line.

able to produce higher resolution radargrams and height profiles (see Figure 5, panel 'a-b-c') that can be diagnostic of the process(es) responsible for sharp-edged depressions formation. In particular, the width of the raised rims and their internal/external steep slopes can be characterized now with higher precision [26].

IV. Conclusion

This paper proposes a re-processing for the Cassini RADAR altimeter data for improving its along-track resolution by adapting the delay/Doppler algorithm to the Cassini geometry. This algorithm is currently widely applied for Earth observation and its application to the Cassini data provides a most detailed topography for Saturn's largest moon, Titan.

We described how to adapt the delay/Doppler algorithm to the hyperbolic orbits traveled by the Cassini spacecraft during its Titan's flybys, accounting also for the compensation of the antenna mispointing. We showed that up to a tenfold improvement in the along-track resolution is achievable with respect to the conventional processing.

Two case studies, over specific geomorphic units were presented, including hummocks and empty lake basins. These preliminary case studies demonstrated how the improvements provided by the DDA algorithm can advance our knowledge of Titan's surface and will allow for further applications over key geologic features, like equatorial dunes [27], canyons [28] or seas and lakes [29]. The processing techniques discussed herein will result in the release to the scientific community of new altimetry data products that will open a number of research fronts.

Acknowledgment

This research was supported by the Cassini-Huygens mission, a cooperative endeavor of NASA, ESA, and ASI managed by JPL/Caltech under a contract with NASA.

References

[1] C. Elachi, M. D. Allison, L. Borgarelli, P. Encrenaz, E. Im, M. A. Janssen, W. T. K. Johnson, R. L. Kirk, R. D. Lorenz, J. I. Lunine, D. O. Muhleman, S. J. Ostro, G. Picardi, F. Posa, C. G. Rapley, L. E. Roth, R. Seu, L. A. Soderblom, S. Vetrella, S. D. Wall, C. A. Wood, H. A. Zebker, "RADAR: The Cassini Titan radar mapper", Space Sci. Rev., 115(1), 71–110, 2004.

[2] H. A. Zebker, Y. Gim, P. Callahan, S. Hensley, R. Lorenz, "Analysis and interpretation of Cassini Titan radar altimeter echoes", Icarus, Volume 200, Issue 1, Pages 240-255, 2009.

[3] G. Alberti, C. Catallo, L. Festa, E. Flamini, R. Orosei, C. Papa, G. Picardi, R. Seu, F. Spataro, and G. Vingione, The Processing of Altimetric Data (PAD) System for Cassini RADAR, Mem. S. A. It. Suppl., 11, 68, 2007.

[4] E. Montefredini, F. Morelli, G. Picardi, and R. Seu, "A non-coherent surface backscattering model for radar observation of planetary bodies and its application to Cassini radar altimeter", Planet. Space Sci., 43, 1567–1577, 1995.

[5] R. M. C. Lopes, Stofan, E. R., Peckyno, R., Radebaugh, J., Mitchell, K. L., Mitri, G., Wood, C. A., Kirk, R. L., Wall, S. D., Lunine, J. I., Hayes, A., Lorenz, R., Farr, T., Wye, L., Craig, J., Ollerenshaw, R. J., Janssen, M., Legall, A., Paganelli, F., West, R., Stiles, B., Callahan, P., Anderson, Y., Valora, P., Soderblom, L., and Cassini RADAR Team, "Distribution and interplay of geologic processes on Titan from Cassini radar data", Icarus, 205, 540–558, 2010.

[6] P.G. Ford, G.H. Pettengill, "Venus Topography and Kilometer-Scale Slopes", J. Geophys. Res., 97, E8, pp. 13103-13114, 1992.

[7] G. Picardi, R. Seu and S. Sorge, "Extensive non-coherent averaging in Doppler beam sharpened space-borne radar altimeters," Geoscience and Remote Sensing Symposium Proceedings, IGARSS '98, 1998 IEEE International, Seattle, WA, pp. 2643-2645, vol.5., 1998.

[8] R. K. Raney, "The delay/Doppler radar altimeter", IEEE Transactions on Geoscience and Remote Sensing, Vol. 36, No. 5, Sept. 1998.

[9] S. Dinardo, B. Lucas, and J. Benveniste, "Sentinel-3 STM SAR ocean retracking algorithm and SAMOSA model" in *Proc*. 2015 IEEE International Geoscience and Remote Sensing Symposium (IGARSS), Milan, Italy, 2015, pp. 5320-5323.

[10] C. Ray et al., "SAR Altimeter Backscattered Waveform Model," in IEEE Transactions on Geoscience and Remote Sensing, vol. 53, no. 2, pp. 911-919, Feb. 2015.

[11] S. Vignudelli et al., "The COASTALT project: Towards an operational use of satellite altimetry in the coastal zone," in *Proc*. OCEANS 2009, Biloxi, MS, pp. 1-6, 2009.

[12] B. W. Stiles, "Cassini Radar Basic Image Data Records SIS", Version 1.3, JPL D-27889, June 27, 2005. [Online]. Available: https://pds-imaging.jpl.nasa.gov/documentation/Cassini_BIDRSIS.PDF

[13] Skolnik, M., "Radar Handbook", 3rd ed., McGraw-Hill Education, Columbus, Ohio, isbn:9780071485470, 2008.

[14] K. M. Cuomo, "A Bandwidth Extrapolation Technique for Improved Range Resolution of Coherent Radar Data", DTIC Project Report, CJP-60, Rev.1, Dec. 4, 1992. [Online]. Available: http://www.dtic.mil/docs/citations/ADA258462.

[15] M. Mastrogiuseppe, V. Poggiali, A. Hayes, R. Lorenz, J. Lunine, G. Picardi, R. Seu, E. Flamini, G. Mitri, C. Notarnicola, P. Paillou, H. Zebker, "The bathymetry of a Titan sea, Geophys. Res. Lett., 41, 1432–1437, 2014, doi: 10.1002/2013GL058618.

[16] M. Mastrogiuseppe *et al.*, "Radar Sounding Using the Cassini Altimeter: Waveform Modeling and Monte Carlo Approach for Data Inversion of Observations of Titan's Seas", IEEE Transactions On Geoscience And Remote Sensing, Vol. 54, No. 10, 2016, doi: 10.1109/TGRS.2016.2563426

[17] M. Mastrogiuseppe, A. G. Hayes, V. Poggiali, J. I. Lunine, R. D. Lorenz, R. Seu, A. Le Gall, C. Notarnicola, K. L. Mitchell, M. Malaska, S. P. D. Birch, Bathymetry and composition of Titan's Ontario Lacus derived from Monte Carlo-based waveform inversion of Cassini RADAR altimetry data, In Icarus, Volume 300, Pages 203-209, 2018, https://doi.org/10.1016/j.icarus.2017.09.009.

[18] M. C. Raguso, M. Mastrogiuseppe, R. Seu and L. Piazzo, "Super Resolution and Interferences Suppression Technique Applied to SHARAD Data," 2018 5th IEEE International Workshop on Metrology for AeroSpace (MetroAeroSpace), Rome, 2018, pp. 242-246. doi: 10.1109/MetroAeroSpace.2018.8453529.

[19] M. C. Raguso, L. Piazzo, M. Mastrogiuseppe, R. Seu, "Resolution Enhancement and Interference Suppression for Planetary Radar Sounders", Proc. of the 26th European Signal Processing Conference EUSIPCO, pp. 1222-1226, Rome, Italy, 2018.

[20] B. W. Stiles *et al*., "Ground processing of Cassini RADAR imagery of Titan", *2006 IEEE Conference on Radar*, 2006, pp. 8 pp.-. doi: 10.1109/RADAR.2006.1631767

[21] L. C. Wye, "Radar Scattering From Titan And Saturn's Icy Satellites Using The Cassini Spacecraft", Thesis (Ph.D.), Stanford University, 2011. [Online]. Available: https://purl.stanford.edu/fm450ym5976

[22] Bucciarelli, T., Cacopardi, S., Picardi, G., Seu, R., Levrini, G., Perfetti, R. "Tracking Algorithms In Radar Altimetry", International Geoscience and Remote Sensing Symposium (IGARSS'88), vol. 2, Florence, Italy, 973-976 (1988);

[23] R. J. Michaelides, A. G. Hayes, M. Mastrogiuseppe, H. A. Zebker, T. G. Farr, M. J. Malaska, V. Poggiali, and J. P. Mullen, "Constraining the physical properties of Titan's empty lake basins using nadir and off-nadir Cassini RADAR backscatter", Icarus, Volume 270, 2016, Pages 57-66, doi: 10.1016/j.icarus.2015.09.043

[24] A. G. Hayes, S. P. D. Birch., W. E. Dietrich, A. D. Howard, R. L. Kirk, V. Poggiali, M. Mastrogiuseppe, …, C. A. Wood, "Topographic constraints on the evolution and connectivity of Titan's lacustrine basins", Geophysical Research Letters, 44, 11,745–11,753, 2017.

[25] A. G. Hayes, "The Lakes and Seas of Titan", Annual Review of Earth and Planetary Sciences, vol. 44, p.57-83, 2016.

[26] S.P.D. Birch, A.G. Hayes, V. Poggiali, J.D. Hofgartner, J.I. Lunine, M.J. Malaska, S. Wall, R.M.C. Lopes, O. White, "Raised Rims around Ti-

tan's Sharp-Edged Depressions", Geophys. Res. Lett., 45, 2018, doi: 10.1029/2018GL078099
[27] M. Mastrogiuseppe, V. Poggiali, R. Seu, R. Martufi, and C. Notarnicola, "Titan dune heights retrieval by using Cassini radar altimeter", Icarus, 230, 336–354, 2014.
[28] V. Poggiali, M. Mastrogiuseppe, A. G. Hayes, R. Seu, S. P. D. Birch, R. Lorenz, C. Grima, and J. D. Hofgartner, "Liquid-filled canyons on Titan", Geophys. Res. Lett., 43, 2016.
[29] M. Mastrogiuseppe, V. Poggiali, A. G. Hayes, J. Lunine, R. Seu, G. Di Achille, and R. Lorenz, "Cassini radar observation of Punga Mare and environs: Bathymetry and composition", Earth and Planetary Science Letters 496, 89–95, 2018.

Valerio Poggiali was born in Genova, Italy, in 1983. He received the M.S. degree in Telecommunications Engineering in 2011 and the Ph.D. degree (cum laude) in Radar and Remote Sensing in 2017 from the University of Rome "La Sapienza". He is a Research Associate at Cornell University, an associate member of the Cassini RADAR team. He was nominated as Associate Team Member of Cassini RADAR Science Team in 2014 and received a Cassini RADAR Team Group Achievement Award from NASA in 2018.

Marco Mastrogiuseppe was born in Atri (TE), Italy, in 1976. He received the B.S., M.S., and Ph.D. degrees in telecommunication engineering from the University of "Sapienza," Rome, Italy, in 2005, 2008, and 2012, respectively. From 2012 to 2014, he was a Research Collaborator with the Dipartimento Elettronica e Telecomunicazione (DIET), LaSapienza University, Rome. Between 2014 and 2016, he has been a Research Associate with the Cornell Center for Astrophysical Science, Cornell University, Ithaca, NY, USA. He is the author of several articles. His research interests include remote sensing, radar system, data processing, and sounder data analysis for planetary exploration. He received a Group Achievement Award from NASA in 2011, SHARAD Science Operation. He was nominated as Associate Team Member of Cassini RADAR Science Team in 2013. He is a team member of the SHARAD experiment on board MRO. Since 2015, he is a Coinvestigator of the NASA project: Radar for Europa Assessment and Sounding: Ocean to Near-surface. In 2018 he joined as a post-doctoral researcher the Geology and Planetary Science Division at the California Institute of Technology (Caltech), Pasadena, CA, USA.

Alexander Gerard Hayes received B.S. degrees in astronomy and astrobiology and the M. Eng. degree in applied physics from Cornell University, Ithaca, NY, USA, and the M.S. and Ph.D. degrees in planetary science from the California Institute of Technology, Pasadena, CA, USA. He is an Associate Professor of Astronomy at Cornell University and Director of the Spacecraft Planetary Imaging Facility. He uses spacecraft-based remote sensing to study the properties of planetary surfaces, interiors, and atmospheres. He is a Participating Scientist on the Cassini-Huygens Mission to Saturn, as well as a Co-Investigator on NASA's Europa Multiple Flyby Mission and the Mars2020 rover. He is a collaborator on the Mars Exploration Rover and Mars Science Laboratory. Dr. Hayes is the winner of the Ronald Greeley Early Career Award of the Planetary Sciences Section of the American Geophysical Union and the Zeldovich Prize in Commission B of the Committee on Space Research. He is also a Kavli Fellow of the National Academy of Sciences and a NASA Early Career Fellow.

Roberto Seu was born in 1959, Italy in Carbonia (CA), Italy. He received the M.S. degree in electronics engineering in 1985 and the PhD. degree in Communications and information technologies engineering in 1990 from the University of Rome "La Sapienza". He is an assistant professor and a lecturer of the course of "Radar systems for space applications" and "Systems for air traffic control" at the Dipartimento di Ingegneria dell'Informazione, Elettronica e Telecomunicazioni of the University of Rome "La Sapienza". He is also a member of the Cassini RADAR team, principal investigator of the Mars SHAllow RADar (SHARAD) sounder on board the NASA mission MRO and co-investigator of the experiment MARSIS, radar sounder on board the ESA mission Mars Express. Dr. seu is a referee of planetary and space science, the IEEE Transactions On Geoscience And Remote Sensing, the IEEE Transactions On Aerospace And Electronic Systems, and of the scientific journal Icarus.

Joseph Peter Mullen was born in Fonda, Iowa in 1993. He received the B.S. degree in astronomy, physics, and mathematics in 2016 from Drake University. He is pursuing a PhD. degree in astrophysics starting fall 2018.

Samuel Patrick Dennis Birch received B.A. degree with honors in Geophysics from University of California Berkeley in 2014 and Ph.D. in Planetary Science (minors: Geophysics/Astronomy) from Cornell University, Ithaca, NY, USA, in 2017. His research is focused on understanding the evolution of the surfaces of planetary bodies. In particular his current research interests involve Titan Polar Geomorphology & Landscape Evolution Modeling, Cometary and Small-Body Surface Processes and Alluvial Fan Dynamics.

Maria Carmela Raguso received her master's degree in Telecommunication Engineering and Ph.D. in Radar and Remote Sensing from University of Rome, "Sapienza", in 2013 and 2018 respectively. In 2018 she joined as a post-doctoral researcher the Geology and Planetary Science Division at the California Institute of Technology (Caltech), Pasadena, CA, USA. Her research interests include the analysis of planetary radar sounder signals (MARSIS and SHARAD) for information extraction purposes and the study of several data processing techniques oriented to improve sounding capabilities and enhance the quality of the sounder radar data products.